# A Combined Experimental and Theoretical Study on Vibrational and Optical Properties of Copolymer Incorporating Thienylene-Dioctyloxyphenyle-Thienylene and Bipyridine Units

**S. Ayachi, S. Ghomrasni, K. Alimi**

*Unité de Recherche, Matériaux Nouveaux et Dispositifs Electroniques Organiques, Faculté des Sciences, Université de Monastir, 5000 Monastir, Tunisie*

Received 4 November 2010; accepted 25 April 2011
DOI 10.1002/app.34743
Published online 31 August 2011 in Wiley Online Library (wileyonlinelibrary.com).

**ABSTRACT:** Optical properties of conjugated copolymer incorporating thienylene-dioctyloxyphenyle-thienylene and bipyridine units prepared by Stille coupling reactions in the ground and lowest singlet excited states were calculated with Time Dependent Density Functional Theory (TD-DFT), CIS/3-21G*, and semiempirical (ZINDO) methods. The complementarities and the good agreement between theoretical and experimental results have permitted us to describe electronic structure and to predict a correlation between structure and properties of this new copolymer. Then, on the basis of these results, we show that this copolymer could be exploited as an active layer in optoelectronic devices. © 2011 Wiley Periodicals, Inc. J Appl Polym Sci 123: 2684–2696, 2012

**Key words:** copolymers; UV–Vis spectroscopy; luminescence; DFT calculations; spectra simulation

## INTRODUCTION

Researches into new conjugated systems with high electro-optical properties have led us to synthesize regular copolymers and polymer blends containing aromatic and hetero-aromatic rings.[1,2] In these categories of materials, copolymers containing both thiophene and phenylene units have also proved to be of interest in combining the properties associated to the two different conjugated rings.[3–5] Pyridine-based conjugated polymers is a promising candidate for light-emitting devices.[6,7] When compared with phenyl-based analogues, one of the most important features of the pyridine-based polymers is the higher electron affinity. Consequently, the polymer is more resistant to oxidation and shows better electron transport properties.[8] According to what have been said before, our research is focused firstly on the synthesis of conjugated copolymers incorporating thiophene and phenylene. In fact, a variety of thienylene-dioctyloxyphenyle-thienylene (as denoted TBT) and bipyridine (BIPY), biphenylene (BIPH) or anthracene (Antra) unit were synthetized.[9,10] Then, experimental results showed that TBT-copolymers have their first optical transition energy values in the visible spectrum and have a good processability as well as interesting electronic properties. Accordingly, these TBT-copolymers seem to be potentially interesting materials for optoelectronic applications. Secondly and before the use of these copolymers as an active layer in optoelectronic devices, we are interested to study deeply their optical properties in order to predict the correlation between structure and properties and to modulate their properties for specific optoelectronic devices.

Concerning this category of these TBT-copolymers, we have firstly interested to complete theoretically their optical properties. Thus, in this article, we carry out a theoretical approach to the optical properties of the TBT-BIPY copolymer performing wide range of calculations and testing their capability to predict the experimental results. The electronic properties as well as the optical absorption and emission spectra were calculated using TD-DFT/3-21G*, CIS/3-21G* levels, and semiempirical quantum-chemical ZINDO approach carried on the ground and excited states. The combination of these methods has been successfully used, in the past, to describe the optical properties of conjugated materials with considerable accuracy.[11,12] With the assistance of quantum chemical calculations, Raman vibrational frequencies have been also calculated and compared with the experimental data.

## EXPERIMENTAL AND THEORETICAL DETAILS

### Experimental measurements

Soluble copolymer alternating A–B-type polymers, when A is the dioctyloxy-substituted phenylene

*Correspondence to:* K. Alimi (kamel.alimi@fsm.rnu.tn).

incorporated between two electron-rich-thiophene untis, abbreviated as TBT unit, and B is a bipyridine (BIPY) unit, was synthesized according to the Stille reaction method and the detailed procedure and characterization were reported elsewhere.[9,10] The molecular structure of the compound is shown in Figure 1. The UV–Visible absorption spectrum of TBT-BIPY copolymer was recorded on a MC2 Safas spectrometer and its photoluminescence spectrum was measured using an SLM-Aminco MC 200 spectrometer. Spectra of TBT-copolymer dissolved in chloroform ($CHCl_3$) were recorded at ambient temperature.

Raman scattering spectrum was recorded by using an excitation laser wavelength of 1064 nm on a Fourier-Transform Raman spectrometer Bruker RFS 100, with a spectral resolution of 4 $cm^{-1}$.

### Method of calculations

First of all, TBT-BIPY copolymer was rendered solution processible by its substitution with dioctyloxy side groups, but it is reasonable to presume that such substitution has little influence on the molecular electronic properties (in particular the energy of the $\pi \rightarrow \pi^*$ electronic transition) that are mainly dependent on the length of the $\pi$-electron system.[13] Accordingly, for our model compound, methoxy groups were used in order to reduce the time of calculation. In this work, geometric structures of TBT-BIPY with two different chain lengths (1 and 2 units) were optimized using the most popular Becke's three-parameter hybrid functional, B3,[14] with nonlocal correlation of Lee-Yang-Parr, LYP, abbreviated as B3LYP, method.[15] This method, based on Density Functional Theory (DFT) for an uniform electron gas (local spin density approximation), is used with the 3-21 G* basis set.[16] This basis set has been successfully applied to some conjugated polymer systems.[17–21]

The electronic properties such as HOMO (Highest Occupied Molecular Orbital), LUMO (Lowest Unoccupied Molecular Orbital) levels, and their corresponding energetic levels difference for TBT-BIPY copolymers are also elucidated. Vibrational Raman

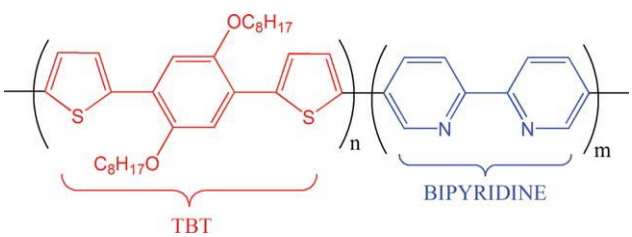


**Figure 1** Chemical structure of TBT-BIPY copolymer. [Color figure can be viewed in the online issue, which is available at wileyonlinelibrary.com.]

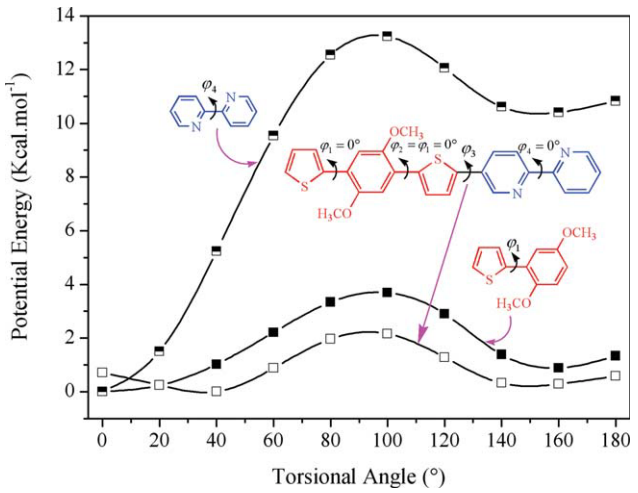


**Figure 2** Torsional potential curves of thienylene-2,5-dimethoxy-phenylene, BIPY, and TBT-BIPY structures obtained at B3LYP/3-21G*. [Color figure can be viewed in the online issue, which is available at wileyonlinelibrary.com.]

frequencies calculation have been carried out with the same method on geometry-optimized structure and directly compared with those of Raman spectroscopy measurements. For the consistency of methodology, the well-known Configuration Interaction Singles (CIS) method[22–25] with 3-21G* is used to optimize the lowest singlet excited-state geometries. All the Time Dependent Density Functional Theory (TD-DFT), the CIS/3-21G*, and the semiempirical quantum-chemical ZINDO levels were used to predict the optical absorption and emission spectra on $S_0$ and $S_1$ optimized structures. Electronic transitions assignment and oscillator strengths were also calculated using the same method of calculations. All calculations reported in this work were carried out with Gaussian 03 program.[26] The simulated absorption and emission spectra were calculated using the SWizard program.[27] Absorption profiles were calculated using Gaussian model (1) with the half-bandwidths ($\Delta_{1/2}$) of 3000 $cm^{-1}$. Vertical transition wavelengths were also done by the same methods.

## RESULTS AND DISCUSSION

### Conformational analysis

Since there was only one type of substitution on the phenyl ring (substitution 2 is equivalent to the site 5), three different conformation types can occur in TBT-BIPY copolymer structure. Then, the potential energy surface (PES) of copolymer was investigated by partial optimization, based on the *ab initio* calculation at the B3LYP/3-21G*. As these structures show flexibility in the molecule, first of all, individual torsion potentials for the two structures of thiophene-di-methoxy-phenylene (TDMP) and bipyridine (BIPY) were obtained for each molecule as a

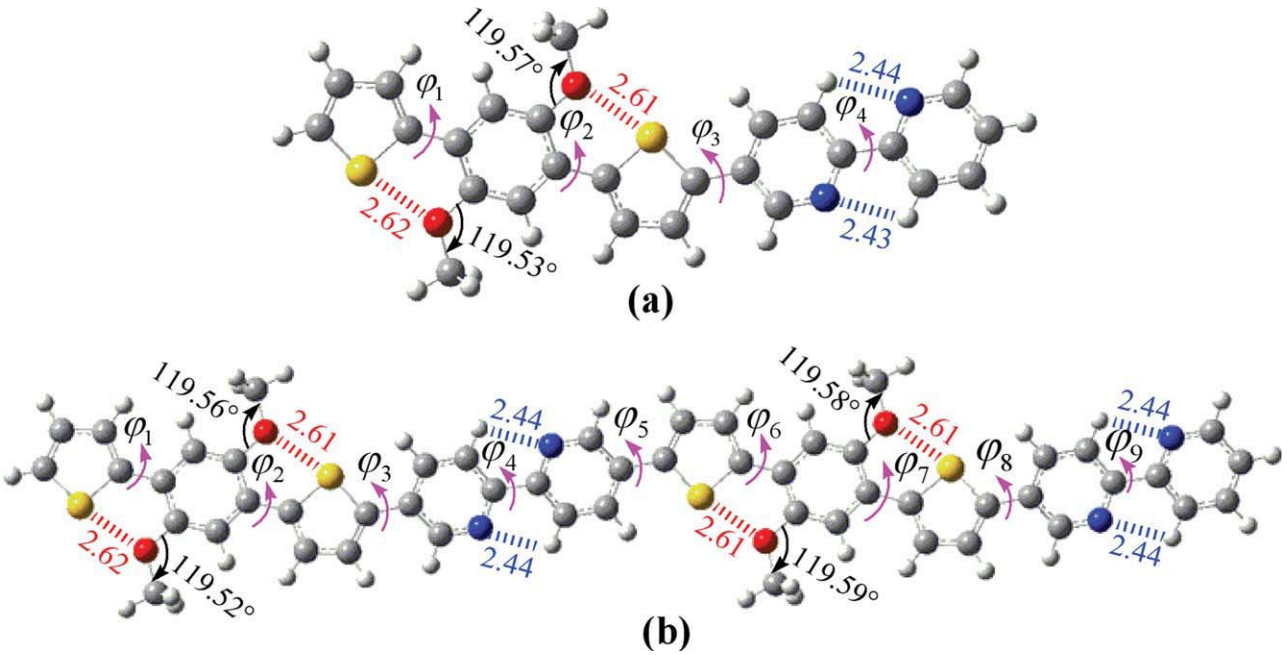


**Figure 3** Ground state B3LYP/3-21G* optimized structures of (a) 1-TBT-BIPY and (b) 2-TBT-BIPY copolymers. [Color figure can be viewed in the online issue, which is available at wileyonlinelibrary.com.]

function of inter-ring C—C dihedral angle $\varphi_1$ (torsional angle between the thiophene and di-methoxyphenylene rings) and $\varphi_4$ (torsional angle between the two pyridine rings) which were varied between 0° (synplanar) and 180° (antiplanar) in 20° steps (Fig. 2). Therefore, to construct the potential energy curve for TBT-BIPY copolymer, $\varphi_1$ and $\varphi_4$ were held fixed, whereas the torsional angle $\varphi_3$ (dihedral angle between the thiophene and pyridine rings) was also calculated in the same way for the previously torsional angles ($\varphi_1$ and $\varphi_4$) determination. For TDMP and BIPY conformational analysis, both showed that there is a global minimum at the torsional angle around 0°, and they adopt coplanar conformations. However, when BIPY is connected to TBT unit, molecule twisted out of the planarity with an angle of $\varphi_3 = 40°$. Accordingly, all the inter-ring dihedral angles $\varphi_1 = \varphi_2 = \varphi_4 = 0°$ and $\varphi_3 = 40°$ were fixed during our geometry optimizations.

### The ground-state geometries of TBT-BIPY copolymers

Density Functional Theory (DFT) method, which is widely used for ground state calculations for π-conjugated systems,[28–32] was employed to optimize the two structures of TBT-BIPY (1 and 2 units or $n = m = 1$ and $n = m = 2$). For simplification, we will call them 1-TBT-BIPY and 2-TBT-BIPY, respectively. The ground-state B3LYP/3-21G* optimized geometry structures are shown in Figure 3. As shown in Table I, the two TBT and bipyrdine units of 1-TBT-

**TABLE I**
**Calculated Torsion Angle and Dihedral Angle in Their Ground and Excited States of TBT-BIPY Copolymers**

| | 1-TBT-BIPY | | 2-TBT-BIPY | |
|---|---|---|---|---|
| Angle (°) | Ground state | Excited state | Ground state | Excited state |
| θ (8,12,13) | 119.57 | 122.25 | 119.56 | 122.28 |
| θ (11,14,15) | 119.53 | 122.41 | 119.52 | 122.27 |
| θ (40,44,45) | – | – | 119.58 | 122.19 |
| θ (43,46,47) | – | – | 119.59 | 122.22 |
| $\varphi_1$ | −0.26 | −0.016 | −0.28 | −0.21 |
| $\varphi_2$ | −0.70 | 0.011 | −0.39 | −0.31 |
| $\varphi_3$ | 23.38 | 21.18 | 23.61 | 20.31 |
| $\varphi_4$ | 0.08 | −0.003 | 0.007 | −0.72 |
| $\varphi_5$ | – | – | −24.52 | −2.42 |
| $\varphi_6$ | – | – | −0.20 | −0.34 |
| $\varphi_7$ | – | – | −0.55 | −0.41 |
| $\varphi_8$ | – | – | 23.86 | 1.85 |
| $\varphi_9$ | – | – | −0.088 | −0.091 |

**TABLE II**
**Atomic Charges of Sulfur, Oxygen, Nitrogen, and Hydrogen Atoms in S—O and N—H Intramolecular Interactions**

| Atoms | Atomic charges (e) | |
|---|---|---|
| | Ground state | Excited state |
| $S_5/O_{14}$ | 0.459/−0.565 | 0.513/−0.757 |
| $S_{20}/O_{12}$ | 0.492/−0.566 | 0.560/−0.759 |
| $N_{25}/H$ | −0.619/0.220 | −0.764/0.287 |
| $N_{28}/H$ | −0.619/0.219 | −0.767/0.287 |
| $S_{37}/O_{46}$ | 0.494/−0.565 | 0.568/−0.760 |
| $S_{52}/O_{44}$ | 0.494/−0.565 | 0.569/−0.760 |
| $N_{57}/H$ | −0.618/0.220 | −0.767/0.286 |
| $N_{60}/H$ | −0.605/0.221 | −0.753/0.288 |

BIPY adopt planar conformations with dihedral angles inferior to 1°. Furthermore, we note the same trends for the 2-TBT-BIPY copolymer, in which dihedral angles in the repeated TBT or Bipyridine units does not exceed 1° (Table I). Whereas, the dihedral angles $\varphi_3$ for 1-TBT-BIPY, $\varphi_3$, $\varphi_5$, and $\varphi_8$ for 2-TBT-BIPY are twisted out of plane of ∼ 24°. Then, it is worth noting that attractive interaction forces taking place between the oxygen atom (negatively charged) and the sulfur atom (positively charged) in the TBT unit.[33–35] Similar results were found for the Bipyridine unit, in which intramolecular interaction between nonbonded nitrogen and hydrogen atoms was occurred (the atomic charges are illustrated in Table II). In fact, the determined distance S--O (N--H) of ∼ 2.62 Å (∼ 2.44 Å), which correspond to ∼ 79% (∼ 92%) of the sum of their Van der Waals radii, fall inside the Van der Waals contact distance of the S--O (3.32 Å) and N--H (2.64 Å) and outside of their covalent contacts of 1.70 Å for S—O and 0.91 Å for N—H. In that case, the planar conformations

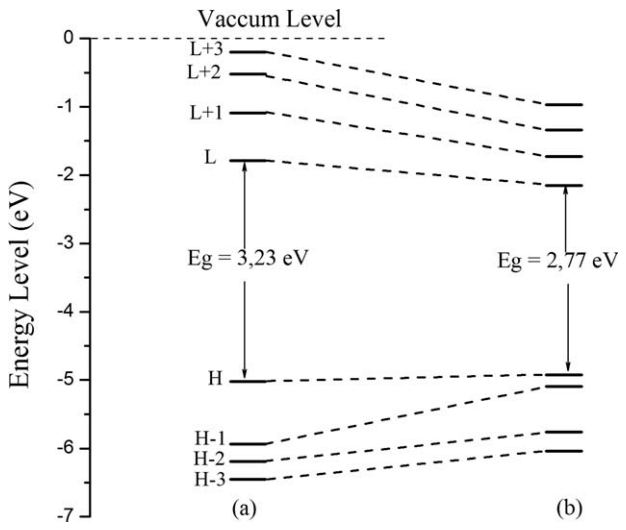


**Figure 4** The DFT//B3LYP/3-21G* calculated energy levels for TBT-copolymers with two different chain lengths: (a) 1-TBT-BIPY and (b) 2-TBT-BIPY.

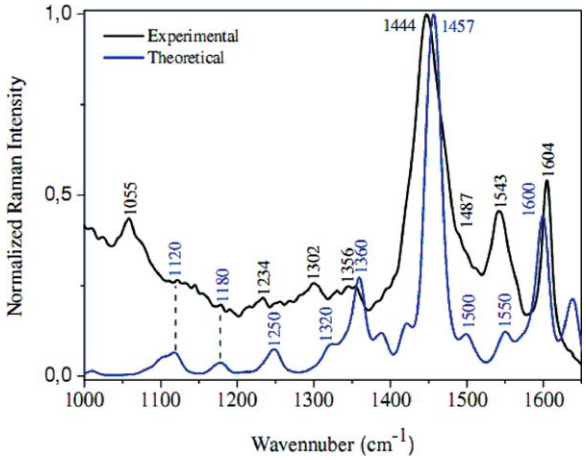


**Figure 5** Experimental and theoretical normalized Raman spectra of TBT-BIPY copolymer. [Color figure can be viewed in the online issue, which is available at wileyonlinelibrary.com.]

are stabilized by the nonbonded S--O and N--H interactions.[36] In addition, the C—O—C angles for both TBT-copolymers are not affected along the polymer chains and are evaluated to be 119.5°.

Furthermore, the highest occupied molecular orbital (HOMO), lowest unoccupied molecular orbital (LUMO), as well as the HOMO-LUMO energy gap ($\Delta_{LUMO\text{-}HOMO}$) were examined. Accordingly, for 1-TBT-BIPY, the HOMO is at −5.019 eV and the LUMO at −1.786 eV, whereas for 2-TBT-BIPY, values obtained are −4.922 eV for the HOMO and −2.152 eV for the LUMO. The LUMO and HOMO levels of 2-TBT-BIPY were found to lie within the HOMO-LUMO gap of 1-TBT-BIPY (∼ 3.23 eV). Consequently, the LUMO level energy significantly decreases is responsible to the optical gap reduction from 3.23 eV (1-TBT-BIPY) to 2.77 eV (2-TBT-BIPY). As a result, the energy gap decreases suggesting the maximum absorption peak in UV–Vis spectra will red shift.

To further understand the optical property changes, Figure 4 compares the four highest occupied and four lowest unoccupied orbital levels for the 1- and 2-TBT-BIPY copolymers. It is interesting to note that the HOMO energy levels increase, whereas the LUMO levels decrease for the 2-TBT-BIPY, when compared with those of 1-TBT-BIPY.

On the basis of geometry optimization of the 1-TBT-BIPY, we have calculated vibrational Raman frequencies. Note that for 2-TBT-BIPY units, the Raman frequencies require significantly more computational effort than that is needed for the one TBT-BIPY unit. For that reason, we do not perform calculation for the two TBT-BIPY units.

In Figure 5, we have plotted the normalized theoretical and experimental Raman spectra of the compound. It is relevant to note that vibrational spectrum calculated with the DFT methodology satisfactorily

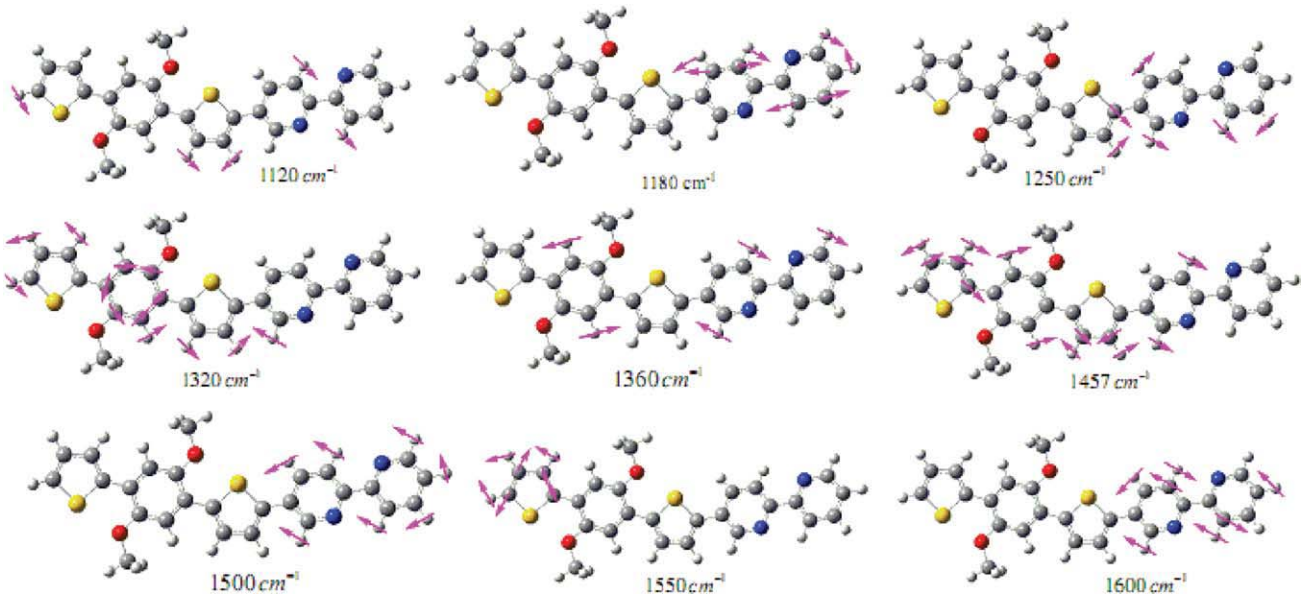


**Figure 6** Selected Raman vibrational modes of the calculated frequencies of 1-TBT-BIPY copolymer. [Color figure can be viewed in the online issue, which is available at wileyonlinelibrary.com.]

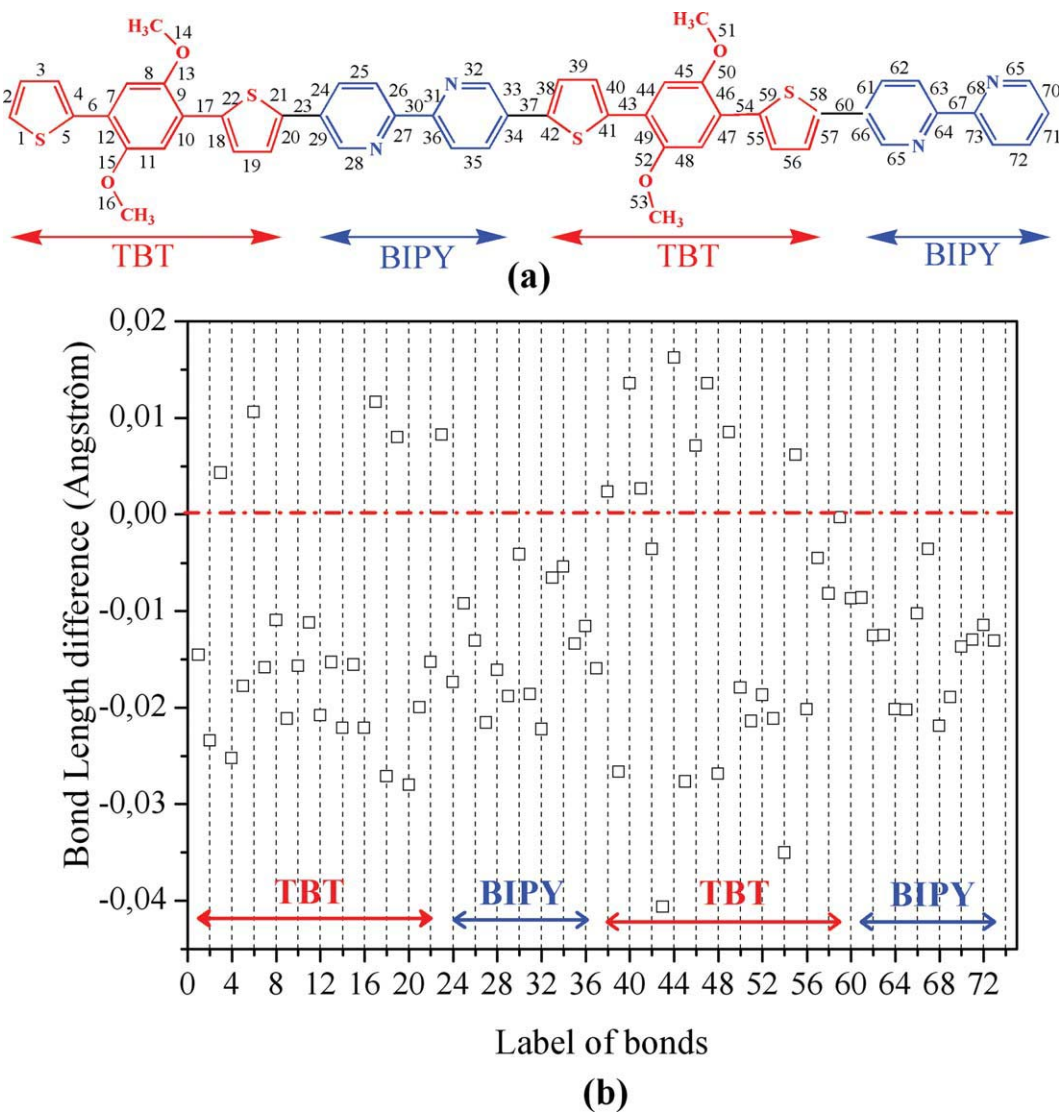


**Figure 7** (a) Structure and bond length numbering of 2-TBT-BIPY copolymer and (b) the difference in bond length between the excited and ground states for the 2-TBT-BIPY copolymer. The horizontal axis labels represent bond between adjacent atoms in the numbering sequence shown in (a). [Color figure can be viewed in the online issue, which is available at wileyonlinelibrary.com.]

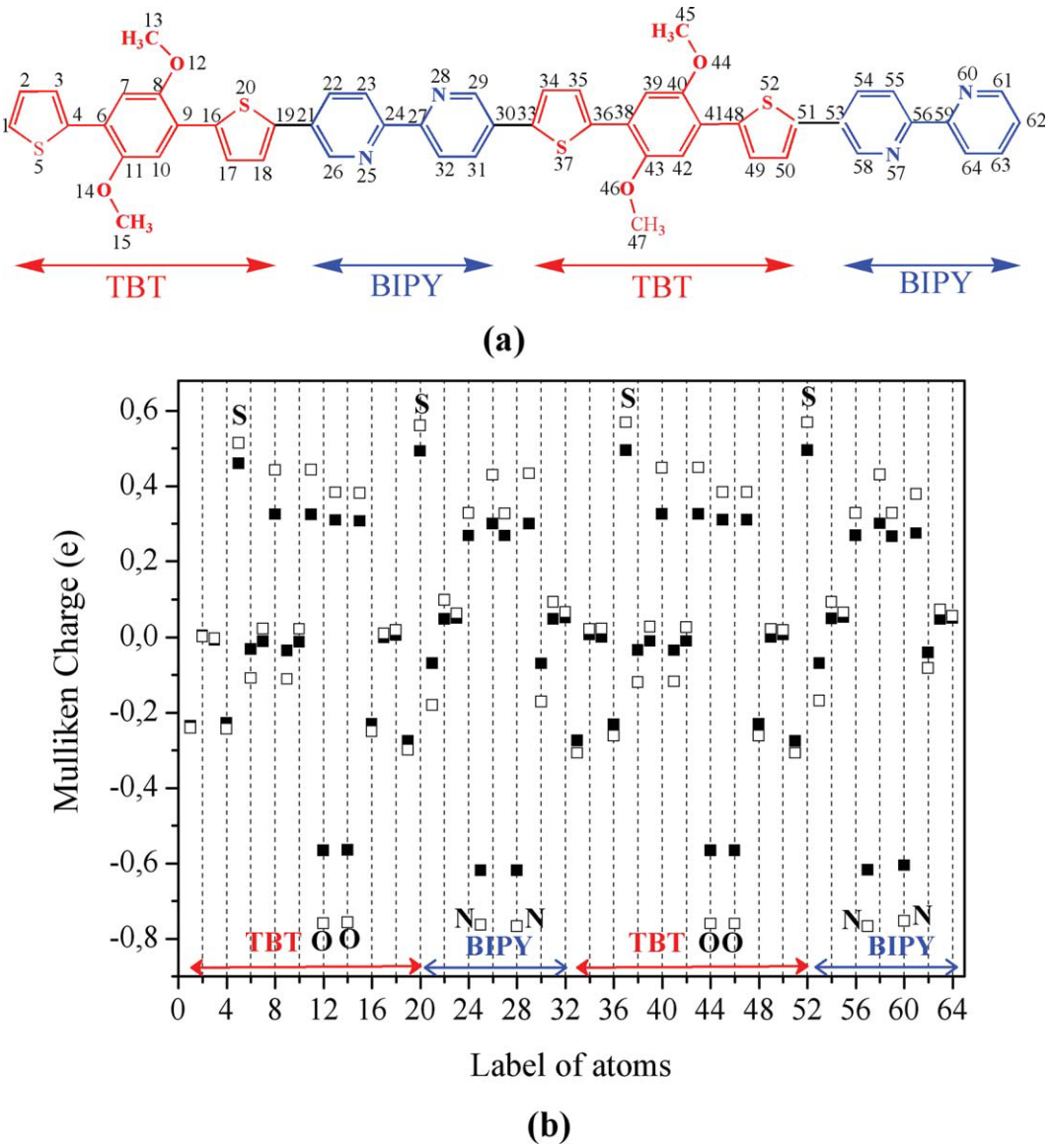


**Figure 8** (a) Structure and atom numbering of 2-TBT-BIPY copolymer and (b) the comparison of the atomic charge (atomic charges with hydrogen's are summed into heavy atoms) for the 2-TBT-BIPY copolymer at the ground (■) and excited (□) states. The horizontal axis labels represent the individual atoms in the numbering sequence shown in (a). [Color figure can be viewed in the online issue, which is available at wileyonlinelibrary.com.]

agree with experimental spectrum both in relative intensities and peak positions. Then, the deviation between measured Raman scattering and the theoretically vibrational frequencies are less than 30 $cm^{-1}$. Moreover, it was found that there were no negative vibrational frequencies, which indicate that optimized structure was at the energy minimum. This implies that the theoretically determined structure of copolymer is the most accurate description of the electronic structures. Accordingly, the Raman bands in the region 1440–1460 $cm^{-1}$ which are assigned to the thiophene ring vibrations[37,38] are strongly resonant with the $\pi \rightarrow \pi^*$ electronic transition of compound. In Figure 6, the most important Raman vibrational modes are collected.

By referring to the experiment optical gap, estimated from the onset of the absorption spectrum, which is $\sim$ 2.43 eV[10] and 0.34 eV deviates from the theoretical ones, we consider that the 2-TBT-BIPY copolymer was firstly used as model structure for predicting the optical and emission properties.

### The excited-state geometries of TBT-BIPY copolymers

The Configuration Interaction Singles (CIS) method with 3-21 G* was used to optimize the lowest singlet excited-state geometries for the two TBT-BIPY copolymers. In this section, we are firstly interested to compare the resulting changes in bond lengths

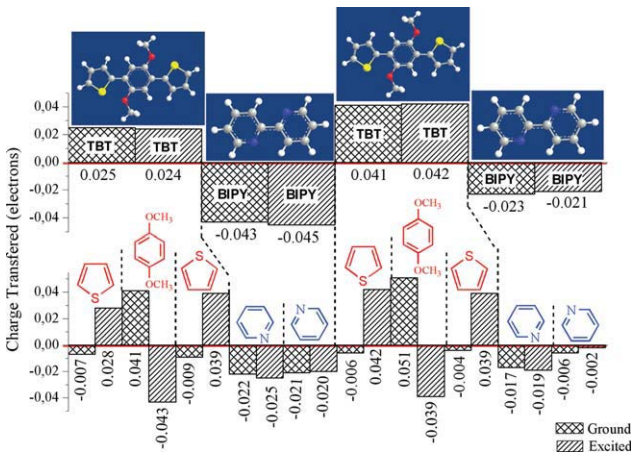


**Figure 9** Illustration of the 2-TBT-BIPY copolymer structure with Mulliken charges distributions for TBT and BIPY units at the ground and excited states. [Color figure can be viewed in the online issue, which is available at wileyonlinelibrary.com.]

and atomic charges deriving a first picture of the extent of localization induced on excited structure. The comparison of the bond lengths and the atomic charge distributions, for the 2-TBT-BIPY copolymer, in their ground and excited states were shown in Figure 7(b) and 8(b), respectively. Thus, the interpretation is based on the bond between adjacent atoms and individual atoms in the numbering sequence presented in Figure 7(a) and 8(a), respectively. As shown in Figure 7(b), that some of bond length lengthened, but some shortened. In the excited $S_1$ state, we note firstly that all the bond lengths of the two bipyridine as well as those of C—O—C are shortened. Whereas, in the left TBT unit, the C—C single bond of thiophene rings as well as that connects the thiophene ring to the phenylene and bipyridine rings increase. Besides, in the second TBT unit, double bonds of thiophene ring and single/double bonds of substituted phenylene ring are also

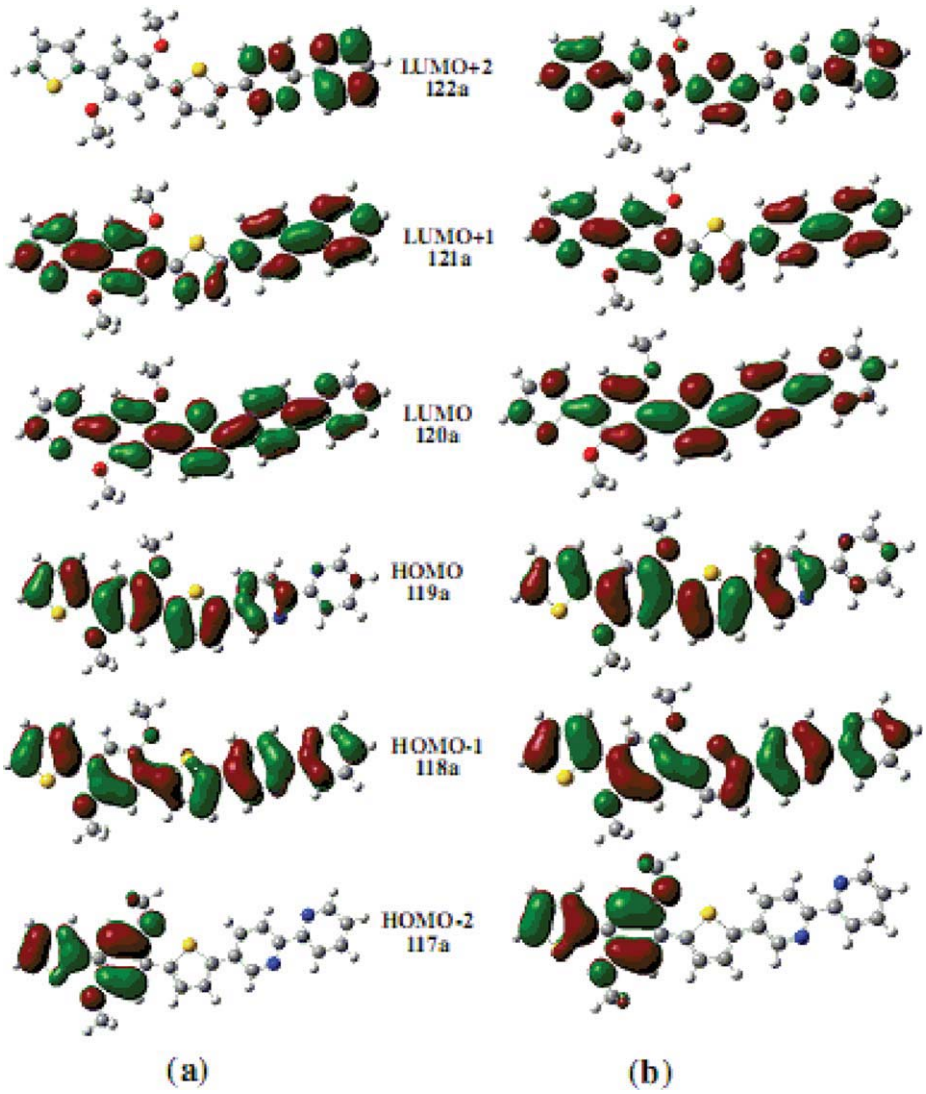


**Figure 10** Frontier molecular orbitals significantly contributing to the electronic transitions of 1-TBT-BIPY copolymer: (a) ground and (b) excited states. [Color figure can be viewed in the online issue, which is available at wileyonlinelibrary.com.]

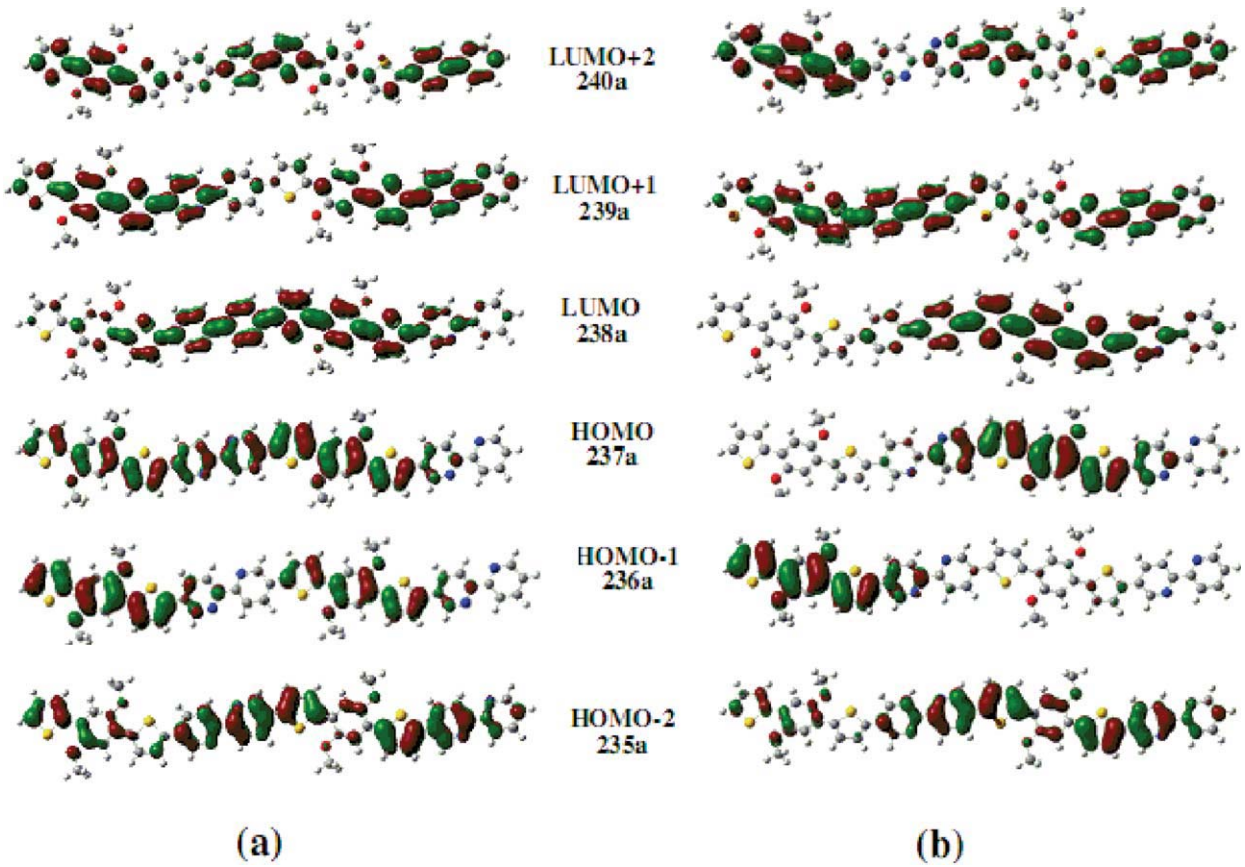


**Figure 11** Frontier molecular orbitals significantly contributing to the electronic transitions of 2-TBT-BIPY copolymer: (a) ground and (b) excited states. [Color figure can be viewed in the online issue, which is available at wileyonlinelibrary.com.]

increased. Additionally, all the C—O—C angles were increased upon excitation (Table I). Whatever the state is, the nonbonded S--O and N--H contacts were found to be considerably shorter than the sum of their Van der Waals radii. These distances vary from $\sim$ 2.62 Å to $\sim$ 2.64 Å (S--O) and from $\sim$ 2.43 Å to $\sim$ 2.46 Å (N--H), when passing from the ground to the excited states. Thus, confirming the occurrence of noncovalent intramolecular interactions. We believe that attractive interaction forces can modify the C—O—C angles in the excited state. Moreover, compared with the 1-TBT-BIPY geometry structure, it is found that 2-TBT-BIPY almost reaches planarity in the excited state.

By analyzing the atomic charge distributions [Fig. 8(b)], a significant negatively charges located on oxygen (nitrogen) in the TBT (bipyridine) units and positively charges located on sulfur atoms in the TBT units were detected upon excitation (Table II). We note, further, that a significant positively (negatively) charges in their first neighboring carbons were also detected. Moreover, no significant changes in all carbons atomic charges in thiophene rings were appreciated. For a good interpretation of these results, a schematic representation for the intramolecular charge transfer (CT) at the ground and excited states of 2-TBT-BIPYcopolymer, calculated as the average of the summation of Mulliken charges distribution of the TBT and BIPY units, is displayed in Figure 9. In general, intramolecular charge transfer is generated through the alternating donor–acceptor conjugated systems.[39] From this figure, we think that the alternating TBT (positively charged) and BIPY (negatively charged) of the model compound are considered as donor and acceptor, respectively. Then, we have separately examined their HOMO and LUMO energetic levels. Findings indicate that for the TBT unit, the HOMO is at −4.29 eV and the LUMO at −1.29 eV, whereas for Bipyridine unit, values obtained are −6.52 eV for the HOMO and −1.33 eV for the LUMO. Although the LUMO energetic levels are quite similar, a weak intramolecular charge transfer in these molecules can be established.

On the basis of the comparison between ground and excited-state geometries for 2-TBT-BIPY, we deduce that the charge distributions are predominantly restricted to the substituted phenylene and thiophene units (Fig. 9). We can also predict the geometry structure changes between the ground ($S_0$) and singlet excited ($S_1$) from molecular orbital

**TABLE III**
**The Vertical Excited Energies (nm) and Their Oscillator Strengths for the Ground ($S_0 \rightarrow S_1$) and First Excited ($S_1 \rightarrow S_0$) States of TBT-BIPY Copolymers by Using CIS/3–21G*, TD//B3LYP/3–21G*, and ZINDO Methods**

| 1-TBT-BIPY copolymer | | | | | | | | | |
|---|---|---|---|---|---|---|---|---|---|
| | Optical absorption properties of ground state ($S_0 \rightarrow S_1$) | | | | Emission properties of excited state ($S_1 \rightarrow S_0$) | | | | |
| Method of calculation | λmax (nm) | Oscillator strength | MO/Character | Coefficient (%) | λmax (nm) | Oscillator strength | MO/Character | Coefficient (%) | Stokes shift (nm/eV) |
| CIS | 312.5 | 2.068 | H→L | 79 | 364.3 | 2.132 | L→H | 85 | 51.8 (0.56 eV) |
| | | | H-1→L+1 | 7 | | | L+1→H-1 | 5 | |
| TD-DFT | 418.3 | 1.410 | H→L | 85 | 464.2 | 1.728 | L→H | 79 | 45.9 (0.29 eV) |
| ZINDO | 434.0 | 1.542 | H→L | 62 | 476.7 | 2.902 | L→H | 84 | 42.7 (0.25 eV) |
| | | | H-1→L+1 | 19 | | | | | |
| | | | H-2→L+2 | 6 | | | | | |
| 2-TBT-BIPY copolymer | | | | | | | | | |
| | Optical absorption properties of ground state ($S_0 \rightarrow S_1$) | | | | Emission properties of excited state ($S_1 \rightarrow S_0$) | | | | |
| Method of calculation | λmax (nm) | Oscillator strength | MO/Character | Coefficient (%) | λmax (nm) | Oscillator strength | MO/Character | Coefficient (%) | Stokes shift (nm/eV) |
| CIS | 357.2 | 4.364 | H→L | 60 | 398.7 | 3.055 | L→H | 80 | 41.5 (0.36 eV) |
| | | | H-1→L+1 | 22 | | | L+2→H-2 | 5 | |
| | | | H-2→L+2 | 9 | | | | | |
| TD-DFT | 481.6 | 2.943 | H→L | 78 | 508.8 | 3.224 | L→H | 82 | 27.2 (0.13 eV) |
| ZINDO | 439.4 | 3.781 | H→L | 81 | 519.2 | 4.352 | L→H | 89 | 79.8 (0.43 eV) |
| | | | H-1→L+1 | 5 | | | | | |
| Experimental | | | 436 nm | | | | 498–27 nm | | 62 (0.35 eV) |

(H = HOMO, L = LUMO, L+1 = LUMO+1, etc.)

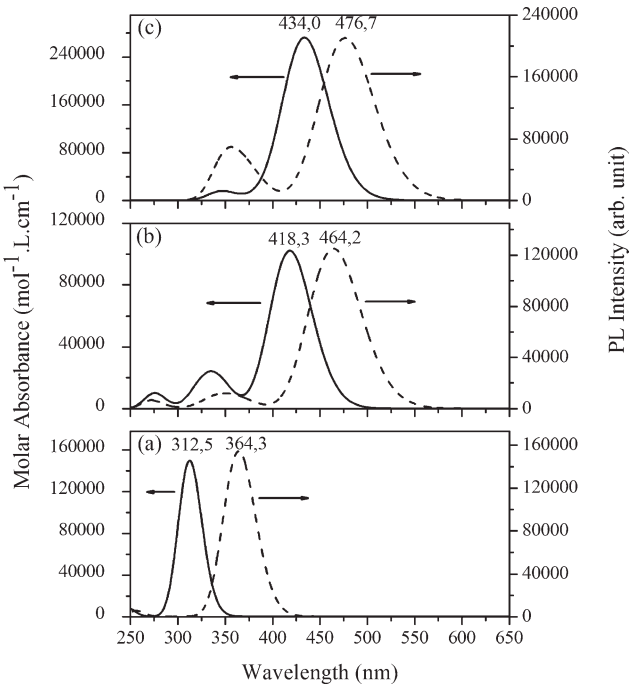


**Figure 12** The simulated optical absorption and emission spectra of 1-TBT-BIPY copolymer with CIS/3-21G* (a), TD-B3LYP/3-21G* (b), and ZINDO (c) methods.

patterns. Then, to better understand the excitation process in TBT-BIPY copolymers, we have investigated the molecular orbital involved in the electronic transition. The frontier molecular orbitals significantly contributing to the electronic transitions of 1-TBT-BIPY and 2-TBT-BIPY, for the ground and excited states, were drawn in Figures 10 and 11, respectively. First, we have separately examined and found that the presence of methoxy side chain does not have a significant effect on the molecular orbital distribution. In the HOMO orbital representation, the C=C segments are π-bonding and have antibonding phase with respect to their neighboring C=C units. Whereas, in the case of the LUMO orbital, the C=C units are antibonding and bonding in the bridge single bond. From Figure 10, we deduce that the frontier orbital spread over the whole π-conjugated backbone in the short chain of copolymer (1-TBT-BIPY). In general, excitation of π-electron from HOMO to LUMO leads to increase localization of electron density on the acceptor part of the molecule. Here, the promotion of one electron from HOMO to LUMO is explained by the frontier molecular orbital. For the two TBT-BIPY copolymers, the LUMO favors the inter-ring mobility of electrons, whereas the HOMO only promotes the intraring mobility of electrons.[40] For the sake of comparison, the HOMO/LUMO molecular orbitals of 2-TBT-BIPY (Fig. 11) were significantly affected (in particular the left TBT unit) indicating their contribution for the excitation processes.

### Electronic transition, optical and emission spectra of TBT-copolymers

We have performed a variety of theoretical approach including CIS/3-21G*, TD-B3LYP/3-21G*, and ZINDO methods to describe optical and emission properties of TBT-BIPY copolymer. Thus, the theoretical results will be compared with the experimental one.

From theoretical calculations, the main wavelengths having the largest oscillator strength as well as their corresponding molecular orbital character for the ground state ($S_0 \rightarrow S_1$) and the first excited state ($S_1 \rightarrow S_0$) using the three above mentioned methods, for 1-TBT-BIPY and 2-TBT-BIPY are listed in Table III. The experimental optical absorption and emission wavelengths maximum for TBT-BIPY copolymer in chloroform solution are also listed in the same table. Clarke et al.[41] suggest that the importance of the HOMO-LUMO transition may be easily understood from the spectral distribution of molecular orbitals. It is argued that to a first approximation, significant overlap between HOMO and LUMO implies an intense transition between HOMO and LUMO and *vice versa*. Here, the vertical $S_0 \rightarrow S_1$ transition was dominated by the H→L excitation (60–81%).

From Table III, we note that the calculated optical absorption wavelengths obtained by using TD-DFT or CIS/3-21G* deviates the experimental data, which proves that these methods are not accurate to reproduce optical properties for large π-conjugated

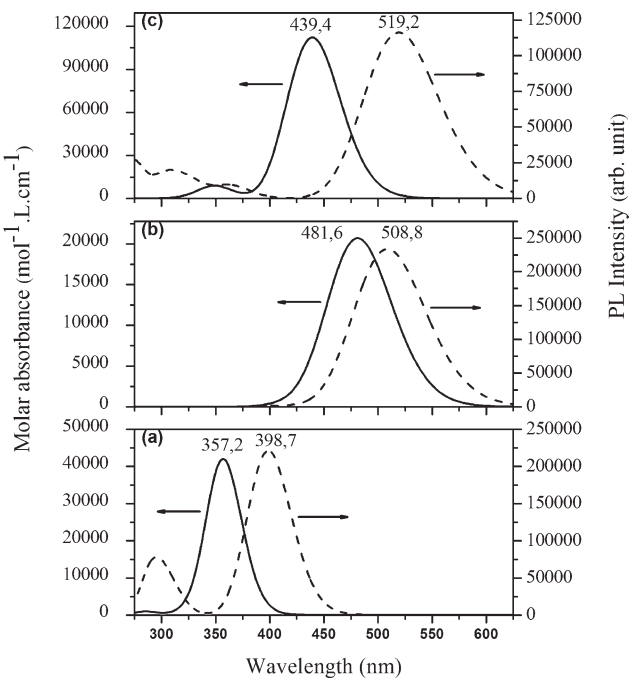


**Figure 13** The simulated optical absorption and emission spectra of 2-TBT-BIPY copolymer with CIS/3-21G* (a), TD-B3LYP/3-21G* (b), and ZINDO (c) methods.

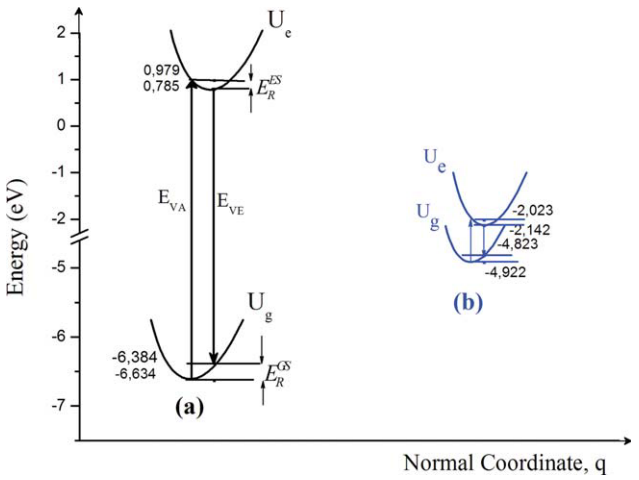


**Figure 14** Schematic representation of the potential energy surface (PES) of the ground ($U_g$) and excited ($U_e$) states along the normal mode coordinate of 2-TBT-BIPY copolymer, using CIS/3-21G* (a) and TD//B3LYP/3-21G* (b) methods. The parameters indicated are the vertical absorption energy ($E_{VA}$), the vertical emission energy ($E_{VE}$), and the relaxation energies ($E_R^{GS}$, $E_R^{ES}$). [Color figure can be viewed in the online issue, which is available at wileyonlinelibrary.com.]

systems.[42–44] Then, it is well known that the failure of TD-DFT in the large systems is attributed to the fact that the exchange-correlation potentials generated by the approximate exchange-correlation functional decay too rapidly in the asymptotic region. As a result, the simple extrapolation of oligomer optical properties is also responsible for this deviation. However, the maximum absorption wavelength calculated by using the ZINDO method was evaluated to be 439.4 nm, which well reproduces the experimental ones (436 nm). Additionally, for the 2-TBT-BIPY, the ZINDO calculated emission wavelength (519.2 nm) is close to the experimental result of 498–527 nm.

In Figures 12 and 13, we have depicted the simulated results of the optical absorption and emission spectra for 1- and 2-TBT-BIPY copolymers using the three mentioned methods. With an increase of the chain length of TBT-BIPY, a shift of the absorption and emission peaks to longer wavelengths is observed independently to the use of calculation method,

**TABLE IV**
**The Vertical Optical Absorption Energy ($E_{VA}$), the Vertical Emission Energy ($E_{VE}$), the Relaxation Energies ($E_R^{GS}$, $E_R^{ES}$), and Stokes Shift (SS) Calculated with CIS/3–21G* and TD//B3LYP/3–21G* Methods for 2-TBT-BIPY Copolymer Model Compound**

| | CIS/3–21G* | TD//B3LYP/3–21G* |
|---|---|---|
| $E_{VA}$ (eV) | 7.613 | 2.899 |
| $E_{VE}$ (eV) | 7.169 | 2.681 |
| $E_R^{GS}$ (eV) | 0.25 | 0.099 |
| $E_R^{ES}$ (eV) | 0.194 | 0.119 |
| SS (eV) | 0.444 | 0.218 |

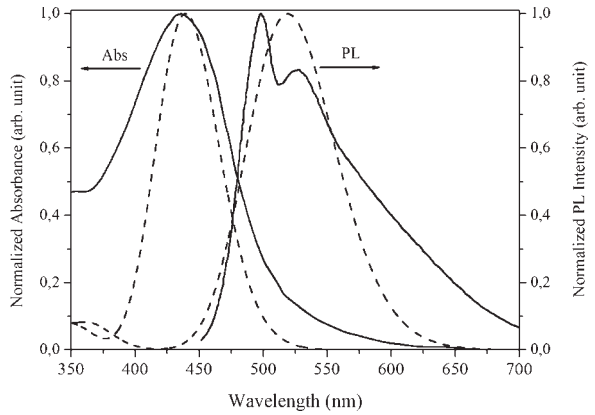


**Figure 15** Normalized experimental optical absorption and photoluminescence spectra of TBT-BIPY copolymer (—) and those calculated at ZINDO method for 2-TBT-BIPY copolymer (- - -).

resulting from the increase of the delocalized conjugation along the backbone of the compounds.[45]

In Figure 14, the two electronic ground and excited states were plotted as two potential energies surface (PES) along the normal coordinate $q$, with the absorption and fluorescence spectra being produced by the transition between these two PES, using CIS/3-21G* and TD-DFT, respectively, for 2-TBT-BIPY copolymer. The vertical optical absorption energy ($E_{VA}$), the vertical emission energy ($E_{VE}$), and in the same way, the relaxation energies ($E_R^{GS}$, $E_R^{ES}$) in the ground and excited states were presented and their corresponding values were reported in Table IV. The stokes shift (SS), which is defined as the difference between the absorption and emission maximums ($E_{VA} - E_{VE}$), is usually related to the band widths of both the absorption and emission bands.[46] It is also a measure of the energy losses due to the molecular relaxation, so it can be expressed as the sum of relaxation energies: $SS = E_R^{GS} + E_R^{ES} = E_{VA} - E_{VE}$.

From Table IV, the CIS/3-21 G* calculated stokes shift (SS) is about two times higher than that calculated with TD-DFT method. Accordingly and due to the neglect of the effects of electron correlation and higher order excitations, the geometry relaxation after excitation contribute much to the stokes shift when using CIS/3-21 G*. It is well known that vertical absorption energy ($E_{VA}$) is usually considered the maximum in the absorption spectrum, but more exactly it must be corrected for the zero-point vibrational energy (ZPE). In our case and compared with the results resorted from spectra simulation (Table III), the calculated stokes shift values (Table IV) deviate by 0.084 eV and 0.088 eV when using CIS/3-21G* and TD-DFT methods, respectively. Accordingly, this difference of around 0.08 eV probably represents the value that will be used subsequently to correct the experimental data. Taking into account

this correction, the experimental value was an excellent estimation to that calculated by ZINDO method (Table III) for the 2-TBT-BIPY copolymer model compound.

To make easy the interpretation of the ZINDO calculated optical absorption and emission spectra, experiment optical results were presented. All curves are normalized to unity at the respective maximum (Fig. 15). Before we make a brief comment on the comparison of experimental and calculated properties of electronic transitions, we should emphasize that no solvent effects were taken into account in the calculation.

It can be seen that experimental optical absorption spectrum displays only one optical band at around 436 nm, assigned to the $\pi \rightarrow \pi^*$ transition of the conjugated copolymer. The photoluminescence (PL) spectrum of TBT-BIPY displays two maximum at 498 nm and 527 nm. The TBT-BIPY copolymer exhibits emission in the blue–green region. From the spectra shapes, we believe that ZINDO results are in agreement with the experiment spectroscopic data.

## CONCLUSIONS

The effect of dioctyloxy groups grafted on 2 and 5 positions of phenyl ring is clearly seen. Then, the planar conformations of TBT and BIPY units are stabilized by the nonbonded S--O and N--H intramolecular interactions, respectively. As a result, an intramolecular charge transfer for the TBT-BIPY copolymer model compound was proposed.

To complete the experimental optical absorption and emission properties of TBT-BIPY copolymer, CIS/3-21G*, TD-B3LYP/3-21G*, and ZINDO semiempirical methods were performed on the basis of the ground- and excited-state geometries. Electronic absorption and emission spectra of the TBT-copolymers show a red-shift of the maximum wavelengths as the chain length increases from 1-TBT-BIPY to 2-TBT-BIPY. Thus, it is clear that the excitation energy (band gap) of TBT-copolymers decreases with chain length. Correlated to the experimental analyses, the use of DFT molecular orbital energies can help to model electronic transitions of copolymer. Besides, from theoretical calculations, the predicted results could be useful as a guide for designing copolymer in optoelectronic displays.

## References


1. Brédas, J. L.; Cornil, J.; Heeger, A. J. Adv Mater 1996, 8, 447.
2. Pei, J.; Yu, W. L.; Huang, W.; Heeger, A. J. Macromolecules 2000, 33, 2462.
3. Silva, R. A.; Cury, L. A.; Marletta, A.; Guimaraes, P. S. S.; Bouachrine, M.; Lère-Porte, J.-P.; Moreau, J. J. E.; Serein-Spirau, F. J Non-Cryst Solids 2006, 352, 3685.
4. Lère-Porte, J.-P.; Moreau, J. J. E.; Serein-Spirau, F.; Torreilles, C.; Righi, A.; Sauvajol, J. L.; Brunet, M. J Mater Chem 2000, 10, 927.
5. Bouachrine, M.; Lère-Porte, J.-P.; Moreau, J. J. E.; Serein-Spirau, F.; Da Silva, R. A.; Lmimouni, K.; Ouchani, L.; Dufour, C. Synth Met 2002, 126, 241.
6. Gebler, D. D.; Wang, Y. Z.; Blatchford, J. W.; Jessen, S. W.; Lin, L. B.; Gustafson, T. L.; Wang, H. L.; Swager, T. M.; MacDiarmid, A. G.; Epstein, A. J. J Appl Phys 1995, 78, 4264.
7. Wang, Y. Z.; Gebler, D. D.; Lin, L. B.; Blatchford, J. W.; Jessen, S. W.; Wang, H. L.; Epstein, A. J. Appl Phys Lett 1995, 68, 894.
8. Wang, Y. Z.; Gebler, D. D.; Fu, D. K.; Swager, T. M.; MacDiarmid, A. G.; Epstein, A. J. Synth Met 1997, 85, 1179.
9. Bouachrine, M.; Bouzakraoui, S.; Hamidi, M.; Ayachi, S.; Alimi, K.; Lère-Porte, J.-P.; Moreau, J. Synth Met 2004, 145, 237.
10. Ayachi, S.; Alimi, K.; Bouachrine, M.; Hamidi, M.; Mevellec, J. Y.; Lère-Porte, J.-P. Synth Met 2006, 156, 318.
11. Li, Y. Y.; Ren, A. M.; Feng, J. K.; Yang, L.; Sun, C. C. Opt Mater 2007, 29, 1571.
12. Liu, F.; Zuo, P.; Meng, L.; Zheng, S. J Mol Struct: THEOCHEM 2005, 726, 189.
13. Woo, H. S.; Lhost, O.; Graham, S. C.; Bradley, D. D. C.; Friend, R. H.; Quattrocchi, C.; Brédas, J. L.; Schenk, R.; Müllen, K. Synth Met 1993, 59, 13.
14. Becke, A. D. J Chem Phys 1993, 98, 5648.
15. Lee, C.; Yang, W.; Parr, R. G. Phys Rev B 1988, 37, 785.
16. Pietro, W. J.; Francl, M. M.; Hehre, W. J.; Defrees, D. J.; Pople, J. A.; Binkley, J. S. J Am Chem Soc 1982, 104, 5039.
17. Tibaoui, T.; Ayachi, S.; Hamidi, M.; Bouachrine, M.; Paris, M.; Alimi, K. J Appl Polym Sci 2010, 118, 711.
18. Pickholz, M.; Dos Santos, M. C. Synth Met 1999, 101, 528.
19. DiCésare, N.; Belletête, M.; Marrano, C.; Leclerc, M.; Durocher, G. J Phys Chem A 1998, 102, 5142.
20. Geskim, V. M.; Brédas, J. L. Chem Phys Chem 2003, 4, 499.
21. Zhou, X.; Ren, A. M.; Feng, J. K. Polymer 2004, 45, 7747.
22. Foresman, J. B.; Gordon, M. H.; Pople, J. A. J Phys Chem 1992, 96, 135.
23. Yang, L.; Ren, A. M.; Feng, J. K.; Liu, X. D.; Ma, Y. G.; Zhang, H. X. Inorg Chem 2004, 43, 5961.
24. Yang, L.; Ren, A. M.; Feng, J. K.; Ma, Y. G.; Zhang, M.; Liu, X. D.; Shen, J. C.; Zhang, H. X. J Phys Chem 2004, 108, 6797.
25. Yang, L.; Ren, A. M.; Feng, J. K. J Comput Chem 2005, 26, 969.
26. Frisch, M. J.; Trucks, G. W.; Schlegel, H. B.; Scuseria, G. E.; Robb, M. A.; Cheeseman, J. R.; Montgomery, J. A., Jr.; Vreven, T.; Kudin, K. N.; Burant, J. C.; Millam, J. M.; Iyengar, S. S.; Tomasi, J.; Barone, V.; Mennucci, B.; Cossi, M.; Scalmani, G.; Rega, N.; Petersson, G. A.; Nakatsuji, H.; Hada, M.; Ehara, M.; Toyota, K.; Fukuda, R.; Hasegawa, J.; Ishida, M.; Nakajima, T.; Honda, Y.; Kitao, O.; Nakai, H.; Klene, M.; Li, X.; Knox, J. E.; Hratchian, H. P.; Cross, J. B.; Adamo, C.; Jaramillo, J.; Gomperts, R.; Stratmann, R. E.; Yazyev, O.; Austin, A. J.; Cammi, R.; Pomelli, C.; Ochterski, J. W.; Ayala, P. Y.; Morokuma, K.; Voth, G. A.; Salvador, P.; Dannenberg, J. J.; Zakrzewski, V. G.; Dapprich, S.; Daniels, A. D.; Strain, M. C.; Farkas, O.; Malick, D. K.; Rabuck, A. D.; Raghavachari, K.; Foresman, J. B.; Ortiz, J. V.; Cui, Q.; Baboul, A. G.; Clifford, S.; Cioslowski, J.; Stefanov, B. B.; Liu, G.; Liashenko, A.; Piskorz, P.; Komaromi, I.; Martin, R. L.; Fox, D. J.; Keith, T.; Al-Laham, M. A.; Peng, C. Y.; Nanayakkara, A.; Challacombe, M.; Gill, P. M. W.; Johnson, B.; Chen, W.; Wong, M. W.; Gonzalez, C.; Pople, J. A. Gaussian 03, Revision A.1; Gaussian, Inc.: Pittsburgh, PA, 2003.
27. Gorelsky, S. I. SWizard Program; University of Ottawa: Canada, 2009; Available at: http://www.sg-chem.net/.
28. Becke, A. D. J Chem Phys 1993, 98, 5648.
29. Liao, H. R.; Lin, Y. J.; Chou, Y. M.; Luo, F. T.; Wang, B. C. J Lumin 2008, 128, 1373.

30. Seminario, J. M.; Zacarias, A. G.; Tour, J. M. J Am Chem Soc 2000, 122, 3015.
31. Seminario, J. M.; Zacarios, A. G.; Derosa, P. A. J Chem Phys 2002, 116, 1671.
32. Choi, C. H.; Kertesz, M.; Karpfen, A. J Chem Phys 1997, 107, 6712.
33. Meille, S. V.; Farina, A.; Bezziccheri, F.; Gallazzi, M. C. Adv Mater 1994, 6, 848.
34. DiCésare, N.; Belletête, M.; Leclerc, M.; Durocher, G. J Mol Struct: THEOCHEM 1999, 467, 259.
35. Leriche, P.; Frère, P.; Roncali, J. J Mater Chem 2005, 15, 3473.
36. Savitha, G.; Hergué, N.; Guilmet, E.; Allain, M.; Frère, P. Tetrahedron Lett 2011, 52, 1288.
37. Botta, C.; Destri, S.; Porzio, W.; Rossi, L.; Tubino, R. Synth Met 1998, 95, 53.
38. Lin, V.; Grasselli, J. G.; Colthup, N. B. Handbook of Infrared and Raman Characteristics Frequencies of Organic Molecules; Academic Press/Harcourt Brace Jovanovich Publishers: New York, 1989.
39. Wu, P.-T.; Kim, F. S.; Champion, R. D.; Jenekhe, S. A. Macromolecules 2008, 41, 7021.
40. Casanovas, J.; Zanuy, D.; Aleman, C. Polymer 2005, 46, 9452.
41. Clarke, T. M.; Gordon, K. C.; Officer, D. L.; Hall, S. B.; Collis G. E.; Burrell, A. K. J Phys Chem A 2003, 107, 11505.
42. Yang, L.; Feng, J. K.; Ren, A. M. Polymer 2005, 46, 10970.
43. Yang, L.; Feng, J. K.; Liao, Y.; Ren, A. M. Opt Mater 2007, 29, 642.
44. Irving, D. L.; Devine, B. D.; Sinnott, S. B. J Lumin 2007, 126, 278.
45. Li, N.; Jia, K.; Wang, S.; Xia, A. J Phys Chem A 2007, 111, 9393.
46. May, V.; Kühn, O. Charge and Energy Transfer Dynamics in Molecular System; Wiley-VCH: Berlin, 2000.